PAPER • **OPEN ACCESS**

Investigation of the Propulsion Properties of an M-shaped Bending-surface Feather Fan under Different Wind Velocities

To cite this article: Luo Qing *et al* 2019 *IOP Conf. Ser.: Mater. Sci. Eng.* **470** 012001

IOP Conf. Series: Materials Science and Engineering 470 (2019) 012001 doi:10.1088/1757-899X/470/1/012001

Investigation of the Propulsion Properties of an M-shaped Bending-surface Feather Fan under Different Wind Velocities

Luo Qing, Nie Xiaofang※ and Zhou Ximing

Lilienthal laboratory, Beijing Implant Aircraft Co., Ltd.

※2377811041@qq.com

Abstract. Flight speed is an important factor that affects flapping-wing propulsion. This study conducted tests on a self-designed rotatory force-measuring platform and simulated different inflow conditions by changing the rotatory angular velocity. An M-shaped bending-surface feather fan was selected as the test model, and the rotatory platform was rotated at different speeds under different propulsion so that the flapping-wing propulsion at different inflow velocities could be measured. Moreover, the wind speed corresponding to the maximum propulsion was determined. The results show that as wind velocity increases within a certain range, the propulsion first increases, then decreases, and finally increases until reaching a maximum wind velocity value of 7.3 m/s.

1. Introduction

Flapping wing propulsion is a novel propulsion mode that differs from traditional rotary machine propulsion and jet propulsion. In recent years, more attention has been paid to ornithopters and underwater bio-robots, and it was found that flapping-wing propulsion has more advantages. At lower Reynolds numbers, flapping non-stationary motion can provide larger lifting forces and also exhibits higher propulsion efficiency, therefore, flapping-wing air vehicles can achieve long distance flights by consuming less energy [1].

Numerous research groups have investigated the generation mechanism of flapping-wing propulsion. Knoller and Bertz found that flapping wings can produce an equivalent angle of attack, and the projection of the generated normal force along the inflow direction can thus be regarded as the propulsion force [2][3]. Jones et al. experimentally investigated the effects of the flapping wing aspect ratio on propulsion properties [4]. Moreover, Ho et al. conducted related tests on the effects of flapping wing stiffness [5]. Furthermore, Jones et al. developed a flapping-wing system with a wingspan of 1270 mm, in which two pairs of flapping wings at the top and bottom can realize both flapping and pitching motion, and wind tunnel tests were performed [6]. Wang et al., from Dalian University of Technology, adopted a non-stationary dual-time Navier-Stokes (NS) equation for pre-processing and examining the propulsion properties of a two-wing ground-effect propeller [7]. According to their results, the propulsion force and efficiency exhibit a similar variation with velocity, i.e., both propulsion and efficiency can achieve a maximum value by varying the velocity at a fixed frequency. Yu et al. performed numerical simulations to study the aerodynamic performance of a flexible micro-ornithopter and explored the influence of wing stiffness on lifting and propulsion forces [8]. In addition, Qian et al. performed numerical simulations to investigate the effect of flapping thin-plate wings with elastic trailing edges on propulsion [9].

The main factors affecting flapping wing propulsion force and efficiency are flight speed, frequency, flapping amplitude, shape, rules of motion, and bending and torsional deformation of the flapping wings [10]. However, the effect of velocity on flapping-wing propulsion has been poorly investigated. Therefore, to explore the relationship between the flapping-wing propulsion properties and velocity at a fixed flapping frequency, cantilever tests were used in this study and aerodynamic tests were performed on a flapping wing model to investigate propulsion forces at different wind velocities. This study provides a theoretical foundation for the design and practical application of large-propulsion flapping wing feather fans for different cruising velocities.

2. Experimental set up and method

2.1. Experimental set up

Figure 1. Rotary platform for force measurement.

We use the self-designed rotary platform for force measurement to finish this experiment, as shown in Fig. 1, and consists of a supporting structure, spindle, rotary supply circuit, and model mounting plate. The platform is not powered but can freely rotate under the action of external forces, thus achieving the advantages of low friction, stable operation, small volume, and a simple structure. It can also be powered when the platform rotates.

A transmission mechanism was installed on the rotary platform to achieve wing flapping, driven by a 1-kW motor and independently powered by a 5S lithium battery. A crank connecting rod structure was adopted, as shown in Fig. 2, and achieved flapping through the reciprocating up-and-down motions of the flapping rods via a sliding rock. The two flapping rods had an identical length of 1.5 m and were mounted on the platform in a symmetrical pattern.

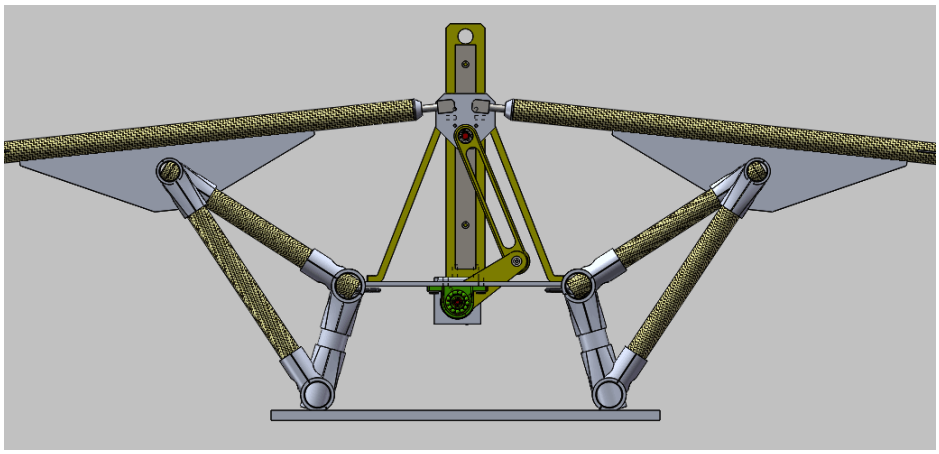

Figure 2. Illustration of the transmission mechanism structure.

A cantilever was fixed on the platform, perpendicular to the flapping rods, and a propeller was installed at a distance of 1.3 m away from the spindle, driven by a 3-kW motor. The motor was powered by a DC supply and provided the rotational power via an electric brush. Once the propeller was switched on, the platform began to rotate and the rotational speed was adjusted by varying the rotational speed of the propeller using a remote controller. The flapping model was mounted on the cantilever and then rotated with the platform while flapping. Therefore, relative motion between the flapping model and air was created and the model was used to simulate the flight process of an ornithopter. The relative velocity between the model and air was calculated based on the angular rotational speed of the platform, and the angular rotating speed was measured using a non-contact tachometer (UT372, UNI-T) with a measurement range of 10~99999 ± 0.04 r/min. The tachometer included a communication module for real-time monitoring via a desktop computer.

2.2. Experimental model

The experimental model was based on the measured propulsion of flapping-wing feather fans with different corners. Since the cantilevers of the rotating force measurement platform flapped up and down, the mounted feather fan model underwent a synchronous movement, and the air on the surface of the feather fan simultaneously exhibited spanwise and chordwise movement. However, the flapping propulsion is a function of the vorticity, mass, velocity, and direction of the shedding vortex, and the spanwise movement of the airflow is perpendicular to the forward direction of the model, and therefore makes no contribution to the flapping propulsion. Assuming the airflow on the surface of the feather fan only exhibis chordwise motion, the airflow disturbances produced during the upward and downward flapping during each flapping cycle develops backwards. In addition, the chordwise vorticity of the shedding vortex resulted in large propulsion magnitudes. On the other hand, spanwise motion of the airflow decreased both the vorticity and mass of the backward-moving shedding vortex, and the propulsion was reduced. Spanwise and chordwise motion of the airflow is illustrated in Fig. 3.

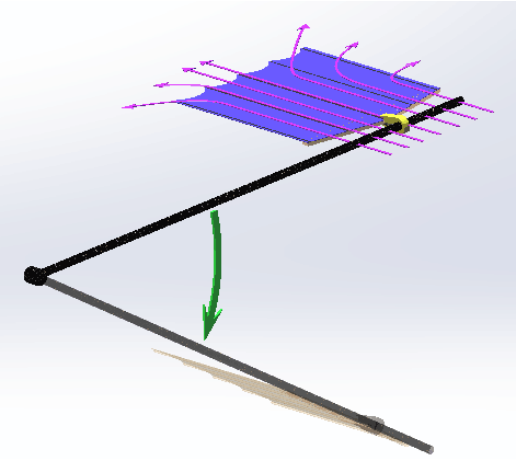

Figure 3. Illustration of spanwise and chordwise motion of airflow.

To avoid spanwise motion, the airflow should move backwards along the chordwise direction. Nine types of flapping weather fans with nine different bending angles (Designed by Lilienthal Laboratory in Beijing Implant Science and Technology Development Co., Ltd.) were used and propulsion was measured at a wind velocity of 15 m/s. The shape and bending angle of the flapping wing feather fan are shown in Fig. 4.

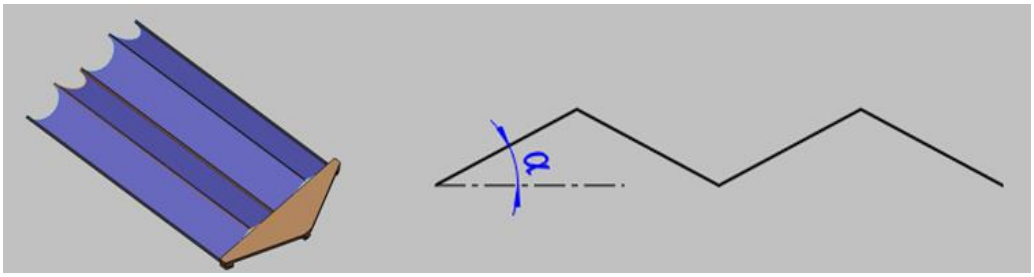

Figure 4. Shape and bending angle of flapping feather fan.

According to the experimental results, an increase of α causes an initial increase in the measured propulsion, followed by a decrease, and the maximum value was reached at α = 12°. This is due to the fact that during the up-and-down flapping wing of the feather fan, the M-shaped groove hinders spanwise motion of the surface airflow and plays the role of chordwise diversion (Fig. 5), therefore, the propulsion increases. When the bending angle exceeded a certain value, the area of the fan increased creating drag, caused by an increase in the chordwise flexible deformation. When α > 12°, propulsion increased. Thus, an M-shaped wing with a bending surface was used as the experimental model in this study.

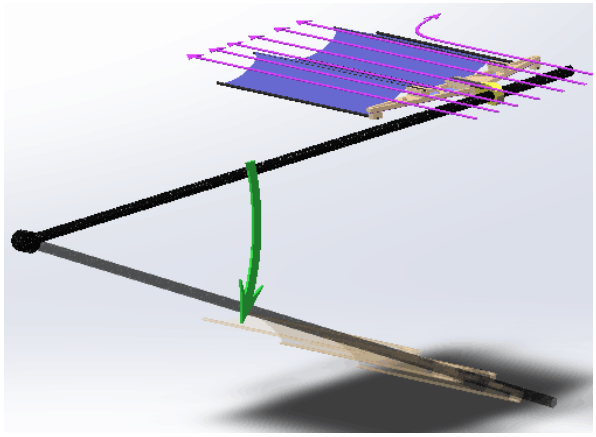

Figure 5. Diversion function of M-shaped feather fan.

As shown in Figure 6, the model consisted of a rectangle with a chord length of 850 mm and a width of 450 mm. The skeleton was composed of five carbon fibre tubes with particular tapering and the tube thickness was 0.4 mm. Ultralight nylon fabric was used as the skin material. The five carbon fibre tubes were alternately arranged along the spanwise direction in a uniformly-spaced pattern, and the angle of intersection between the line connecting adjacent tubes and the plane where the lower pipes were located was 15°, thereby forming an M-shaped bending surface.

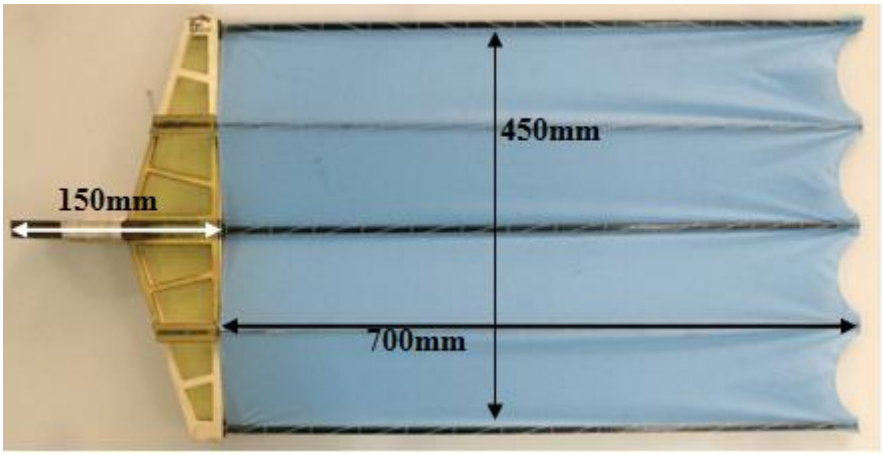

Figure 6. Image of flapping wing feather fan.

2.3. Experimental method

Two flapping-wing feature fans with identical parameters were installed on the flapping rods on both two sides of the platform, at a distance of 1.35 m from the center. The angle of intersection between the feather fan and horizontal plane was zero, and the installation direction was identical to the rotating direction of the platform. First, the flapping frequency was set to 2.5 Hz and the feather fan flapped up and down at a flapping angle of 15°. Then, the platform began to rotate, and the rotational speed of the propeller was adjusted so that the platform could rotate at different angular velocities, allowing for the relative velocity between the feather fan and air to be adjusted. Once the rotational speed of the platform was stable, the flapping stopped and the angular velocity of the rotary platform decreased to a fixed value. The propulsion at a flapping frequency of 2.5 Hz was calculated based on the variation of angular velocity. The preset wind velocity and corresponding angular velocity values are listed in Table 1.

Table 1. Corresponding wind speed and angular velocity values.

Wind velocity (m/s)	Angular velocity at flapping velocity of 2.5 Hz (r/min)
6	42.46
7	49.54
8	56.62
9	63.69
10	70.77
12	84.93
15	106.16

To reduce error, the experiment was repeated 6 times at each wind velocity.

2.4. Experimental principle

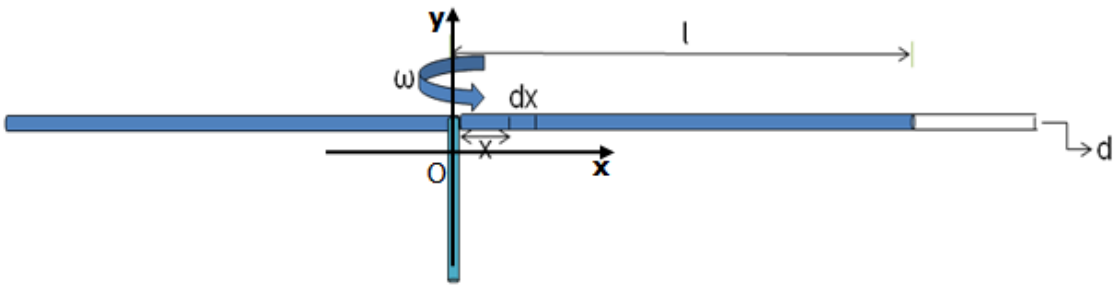

Figure 7. Forces acting on the simplified model.

First, the model was simplified and the applied forces were analyzed without considering flapping.

When the platform rotated at a fixed velocity, the propulsion was equal to the air resistance. Since the platform rotates around its axis, the linear velocities at different points on the rod are different, and the applied resistance exhibits a non-uniform distribution along the length of the rod. The resistance can then be calculated using integration, and a rectangular plane coordinate system can be established, as shown in Fig. 7. An infinitesimal area on the x-axis near the origin was assumed, with the horizontal ordinate denoted as x and the rotating angular velocity denoted as ω. Therefore, the resistance acting on an infinitesimal area can be written as

$$dF = \frac{1}{2}\rho(xw)^2 C_D d * dx \tag{1}$$

$$\frac{1}{2}F = \int_0^l \frac{1}{2}\rho(xw)^2 C_D d * dx \tag{2}$$

$$F = \frac{1}{3} d\rho C_D l \upsilon^2 \tag{3}$$

where l is the length of the cantilever in meters, C_D denotes the average resistance coefficient, ρ is the density of air in kg/m^3, d is the diameter of the cantilever in meters, w denotes the rotatory angular velocity of the platform in rad/s, and υ is the linear velocity of the model installation point in m/s.

In Eq. (3), F is related to C_D. Based on test results, IJ Ritchiek [11] concluded that the resistance coefficient of a smooth cylinder is a function of Reynolds number, i.e., $C_D = f(\mathrm{Re})$. The relationship between the resistance coefficient and Reynolds number is illustrated in Figure 8.

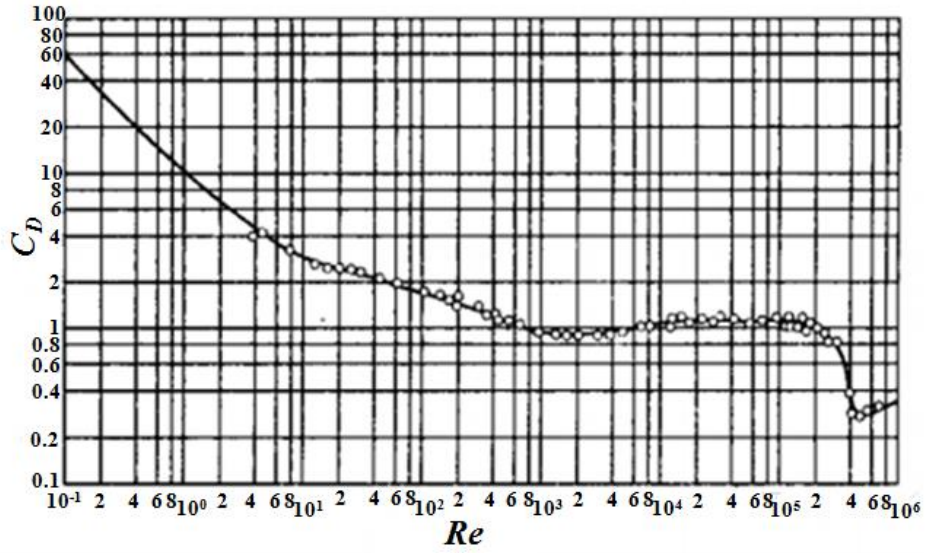

Figure 8. Relationship between resistance coefficient and Reynolds number.

Since the linear velocity of the cantilever at different points from the inside to the outside were different (Fig. 7), in theory, the resistance coefficients on the cylindrical cantilever will also be completely different. Reynolds number can be expressed as

$$\mathrm{Re} = \frac{\rho(xw)d}{\mu} \tag{4}$$

The mean Reynolds number (i.e., the equivalent Reynolds number) on the cantilever can be written as

$$\mathrm{Re} = \frac{1}{l}\int_0^l \frac{\rho w d}{\mu} dx \tag{5}$$

$$\mathrm{Re} = \frac{\rho(\frac{1}{2}lw)d}{\mu} \tag{6}$$

As described in Eq. (6), the Reynolds number at the center of the cantilever is equal to the average Reynolds number. After the value was determined, the corresponding resistance coefficient was acquired from Fig. 8, and resistance was calculated.

Considering that flapping also exists during forward movement of the cantilever, the flapping resistance may vary. Thus, validation tests were performed. After removing the flapping-wing feather fan, tests were conducted according to the method described in Section 1.3. It can be observed that after the flapping stops at a wind velocity of 6 m/s, the linear velocity at the installation point increases by 0.061 m/s. Moreover, as the wind velocity increased to 9 m/s and 10.3 m/s, the linear velocity at this point increased by 0.013 m/s and 0.021 m/s, respectively. Therefore, the effect of flapping on resistance can be neglected.

3. Experimental data and results

Using the rotary platform, linear velocities and average Reynolds numbers of the M-shaped bending-surface feather fan, while flapping or not flapping, were measured at different flow velocities. The results are listed in Table 2.

Table 2. Measured linear velocities and average Reynolds numbers.

Flapping + Propeller (m/s)	Average Reynolds number (Re)	Propeller (m/s)	Average Reynolds number (Re)
6.002	5458.27	4.942	4494.30
7.013	6377.69	6.607	6008.47
8.001	7276.19	7.209	6555.93
8.943	8132.85	8.36	7602.66
9.947	9045.90	9.516	8653.94
11.95	10867.45	11.79	10721.94
15.06	13695.71	14.85	13504.74

Compared to Fig. 8, the resistance coefficient C_D fluctuated only slightly around 1 throughout the test, with a minimum value of 0.9 and a maximum value of 1.1. Therefore, resistance was only related to linear velocity at the installation point of the feather fan. At each wind velocity, the flapping propulsion was calculated by

$$\Delta F = \frac{1}{3} d \rho C_D l (v_1^2 - v_2^2) \tag{7}$$

The form of Eq. (7) is similar to the kinetic energy variation of the system. In other words, flapping led to an increase in the kinetic energy of the system that is proportional to propulsion. According to the test, Δv^2 caused by flapping wing at each wind velocity is shown in Table 3.

Table 3. Linear velocity and Δv^2.

Flapping + Propeller (m/s)	Propeller (m/s)	$\triangle V^2$ (m^2/s^2)
6.002	4.942	11.60064
7.013	6.067	12.37368
8.001	7.209	12.04632
8.943	8.36	10.087649
9.947	9.516	8.388553
11.95	11.79	3.7984
15.06	14.85	6.2811

The relationship between the wind velocity and Δv^2 was plotted, as shown in Fig. 9.

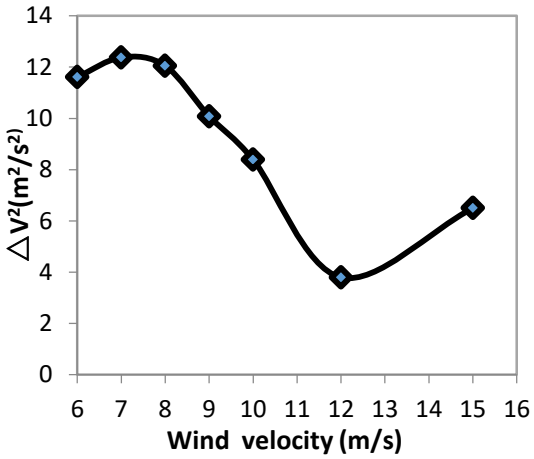

Figure 9. Relationship between wind velocity and $\triangle V^2$.

From Fig. 9, the propulsion of the flapping-wing feather fan first increased and then decreased, finally reaching the maximum at a wind velocity of 7.3 m/s and a minimum at a wind velocity of 12 m/s.

4. Conclusions

(1) As the wind velocity increases, the propulsion of the five-rod M-shaped feather fan first increases and then decreases, followed by a final increase. The optimal wind speed of the flapping-wing feather fan is 7.3 m/s.

(2) Under a particular flapping frequency and stiffness, the flapping-wing feather fan exhibits different degrees of deformation at different inflow velocities, and propulsion of the flapping-wing feather fan reaches a maximum value at an appropriate deformation angle.

(3) The measurement principle of the rotary force-measuring platform was theoretically analyzed, and reliability of the platform was validated. It can also be concluded that, for flapping-wing feather fans of different sizes, shapes, and areas, an optimal inflow velocity exists at which the feather fan can produce maximum propulsion at an optimal deformation angle during the flapping process.

In conclusion, a maximum propulsion velocity exists for each flexible flapping-wing feather fan according to different parameters.

References

[1] Zhang Weiwei, Xu Yang, Jiang Yuewen, et al.Analysis of the characteristics of the flapping-wing propulsion based on the CFD method [J] .Air Dynamics, 2014, 32 (4): 446-452.
[2] Knoller R. Die gesetze des luftwiderstandes[J].Flugund Motortechnik (Wien),1909,3(21):1-7.
[3] Betz, A. Ein beitrag zur erklarung des segeluges[J].zeitschrift fuer Flugtechnik und Motorluftschiffahrt,1912,3:269 – 272.
[4] K. D. Jonesy and M. F. Platzerz [J]. Flapping-wing propulsion for a micro air vehicle. AIAA, 2000.
[5] Steven Ho Unsteady aerodynamics and adaptive flow control of micro air vehicles[D].Los Angeles:University of California 2003:40-52
[6] K. D. Jonesy and M. F. Platzerz [C]. Numerical computation of flapping-wing propulsion and power extraction, Aiaa Aerospace Sciences Meeting and Exhibit. 1997.
[7] Tao W. Performance investigation of symmetrical plunging dual-foils propulsor[J]. Journal of Hydrodynamics, 2009.
[8] Chun-Jin Y U, Hai-Song A. Numerical study of aerodynamics for flexible membrane flapping-wing MAV[J]. Journal of University of Science & Technology of China, 2009, 39(12):1305-1310.

[9] Qian Jing, Zhang Zhengke, Luo Shijun, et al.Numerical study on flow characteristics of two-dimensional elastic flapping wing [J] .Acta Aerodynamica Sinica, 2012, 30 (1): 113-119.
[10] Shao Limin, Song Bifeng, Song Wenping.Experimental Study on Propulsion Characteristics of Micro Flapping Wing [J] .Act on Experimental Hydrodynamics, 2009, 23 (1): 1-6.
[11] IJ Ritchiek, Hydraulic friction manual[M]. Aero Engine Editorial Department, 1985